IEEE Conference on Sensor and Ad Hoc Communications and Networks, October 2004, Santa Clara, USA

An Efficient UWB Radio Architecture for Busy Signal MAC Protocols

Nathaniel J. August and Dong Sam Ha
Virginia Tech VLSI for Telecommunications (VTVT) Lab
Bradley Department of Electrical and Computer Engineering
Virginia Tech, Blacksburg, VA USA 24061-0111
Phone: 530-231-4942; Email: {nateaugu, ha}@vt.edu

***Abstract*— Large wireless ad hoc and sensor networks impose tight constraints on cost and power dissipation, so nodes usually adopt a single transceiver approach. Since a single transceiver cannot assess the status of existing transmissions, it wastes valuable time and energy on handshaking packets and corrupted packets. To avoid such overhead, we propose a single transceiver approach based on ultra wideband (UWB) and a companion medium access control (MAC) layer based on busy tone multiple access (BTMA). BTMA reduces the time and energy spent on collisions as compared to handshaking protocols. It is well suited for ad hoc and sensor networks since it permits random, distributed medium access with no central point of failure. The single transceiver leverages the inherently low duty cycle of impulse-based UWB (I-UWB) to assess the status of a packet during its transmission. This paper describes the I-UWB system architecture, and simulations show that it effectively detects a busy signal without affecting data transmission.**

***Index Terms*—Ultra Wideband, Ad Hoc Networks, Sensor Networks, Medium Access Control, Busy Tone Multiple Access**

I. Introduction

Recent developments in wireless technology have spawned extensive research in wireless ad hoc and sensor networks. Such networks enable various applications such as inventory tracking, home networking, or structural integrity monitoring. These applications demand low power dissipation and low cost. Nodes rely on limited energy resources such as a battery, and the useful lifetime of the network depends on each node's ability to conserve energy. Since these networks may contain a large number of nodes, low node cost is essential to contain the overall network cost.

The medium access control (MAC) protocol and the radio play a crucial role in determining energy dissipation and cost [1]. The radio dictates the energy efficiency and hardware complexity of the physical layer, and the MAC protocol implements the collision avoidance strategy. Collisions and corrupt packets waste energy when packets must be retransmitted. Collisions result from hidden terminals and correlated bursts of traffic. Harsh channel conditions, such as the inside of a ship's metal hull, corrupt packets.

Several research efforts have investigated radios and MAC protocols for ad hoc and sensor networks, and they consider both narrowband and wideband radios [2]-[7]. However, little has been published to exploit the unique capabilities of ultra wideband (UWB) radios or their apposite MAC protocols for large-scale ad hoc and sensor networks.

UWB is a promising radio interface for ad hoc and sensor networks [8], [9]. Impulse based UWB (I-UWB) is particularly attractive due to its resilience to Rayleigh fading from multipath interference, simple transceiver circuitry, accurate ranging ability, and low transmission power [10]-[12]. Resilience to multipath interference permits placement of UWB in areas inhospitable to narrowband systems such as inside metal ship hulls. The carrierless nature of I-UWB results in simple, low power transceiver circuitry, which does not require intermediate mixers and oscillators. The ranging capability allows nodes to accurately (under a centimeter) discern location. Further, UWB is unique in that its radiated power is inherently ultra low as mandated by the FCC maximum of 560 μW, which is at least an order of magnitude less than the radiated power of the systems in [2]-[7].

Large ad hoc and sensor networks impose tight constraints on cost and power, so nodes usually adopt a single transceiver approach. In narrowband or wideband systems, a single transceiver cannot assess the status of existing transmissions, so nodes rely on protocols such as carrier sense multiple access with collision avoidance (CSMA/CA) that use handshaking packets to avoid collisions. In this paper, we propose an I-UWB radio interface with a single transceiver and a companion MAC layer that avoids such overhead.

Our proposed single transceiver leverages the inherently low duty cycle[1] of an I-UWB pulse train to detect collisions and corrupted packets through transmission of a busy signal. The busy signal eliminates handshaking packets such as request-to-send (RTS), clear-to-send (CTS), and acknowledgment (ACK), which can add significant overhead from headers and switching time [13]. Further, since I-UWB systems dissipate far less power transmitting than receiving, the transmission of a busy signal has insignificant impact on the power dissipated in a transaction. The proposed busy signal MAC permits random, distributed medium access with no central point of failure, so it is appropriate for any large ad hoc or sensor network. Also, note that a busy signal MAC provides performance similar to CSMA with collision detection (CSMA/CD), which is more

[1] In this case, the duty cycle refers to the amount of time that the transmitter applies a signal to the antenna during transmission. Duty cycle is also used to describe the cycle of the entire radio through sleep and awake modes.

efficient than CSMA/CA in throughput, delay, and energy per successful transmission [14].

The paper is organized as follows. Section II presents our I-UWB radio design and reviews previous MAC protocols for I-UWB. Section III explains the proposed system architecture and the MAC protocol. Section IV presents simulation results for the proposed system, and Section V concludes the paper.

II. PRELIMINARIES

A. I-UWB Radio Architecture

This section reviews our prior work on an I-UWB receiver and transmitter for the proposed system. I-UWB systems communicate with a train of pulses that have a pulse width on the order of hundreds picoseconds and a bandwidth on the order of gigahertz. The pulse repetition interval (PRI) is generally much longer than the pulse width.

Our transmitter is based on the energy efficient pulse generator in Fig. 1 [11], which can generate various pulse shapes and data rates through a programmable control block. Depending on the desired data rate and pulse shape, the control block adjusts the control voltages C_1, C_2, … C_n to control the direction of current flow and output voltage. The bandpass filter limits the output to the FCC mandated -41.3 dBm/MHz over its bandwidth from 3.1 GHz to 10.6 GHz. The total power from the circuitry is less than 10 μW [11], and the FCC limits the radiated power to 560 μW.

Our receiver employs the frequency domain approach in Fig. 2 [10]. At the front end, a low-noise amplifier (LNA) feeds typical narrowband resonator filters realizing the second order transfer function $1/(s^2+(k\omega_o)^2$. A filter captures an in-band spectral component of the received signal at frequency f_i, where $f_i = kF_0$ for an integer k. The fundamental frequency F_0 is determined by an observation period T_p such that $F_0=1/T_p$. Next, the ADC captures spectral samples at the pulse repetition rate, which is much lower than the Nyquist over-sampling rate to save power as well as circuit complexity. The energy harvester performs baseband signal processing such as the correlation and rake operations in the frequency domain, which results in efficient hardware.

The clear channel assessment (CCA) block in Fig. 2 detects a busy medium in the presence of I-UWB traffic just as carrier sense detects signals in a certain frequency band [15]. The CCA block examines spectral power components to avoid searching for a narrow pulse within a long PRI. When there is pulse activity at the pulse repetition frequency (PRF), the filters oscillate and each energy detector receives a frequency component, f_i, which is an integer multiple of the PRF and T_p. The energy detectors contain an envelope detector followed by an integrator. The outputs of the energy detectors are compared to a threshold and combined to detect the presence of I-UWB pulses, while rejecting narrowband signals.

The transceiver supports data rates from 1 Kbps to 1 Gbps, and it can achieve a bit error rate (BER) of approximately 2×10^{-4} for a link distance of 10 meters in extreme non line-of-sight channel conditions at a data rate of 100 Mbps. Lowering the data rate can increase link distance or improve the BER. The transmitter dissipates less than 600 μW of power [11], which is significantly less than the 200 mW from the receiver.

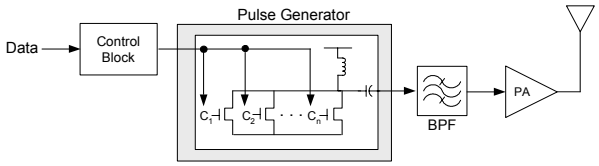

Fig. 1. I-UWB Transmitter

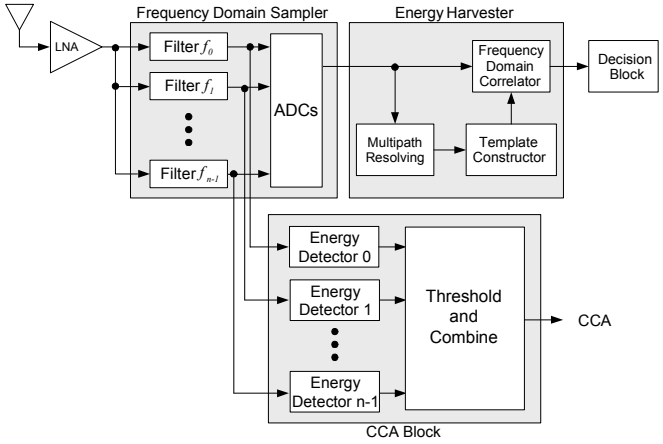

Fig. 2. I-UWB Receiver and Clear Channel Assessment (CCA) Block

B. MAC Protocols for I-UWB

Centralized protocols perform well in terms of throughput, delay, and Quality of Service (QoS), since they collect information about the state of the network. Examples of centralized protocols for I-UWB include the TDMA approach of IEEE 802.15.3a or time hopping [16],[17]. However, centralized protocols add control traffic overhead, have a central point of failure, and require more complex hardware and software.

Distributed protocols are less complex and they scale to large ad hoc or sensor networks. As narrowband systems use carrier sensing to implement random, distributed medium access, I-UWB systems use pulse sense [15]. Pulse sense provides the CCA function for I-UWB. For the receiver in Fig. 2, the pulse sense block performs two important CCA roles. One role is to detect an incoming packet and the other is to ensure that the channel is free before transmitting.

To mitigate the hidden terminal problem, basic PSMA is augmented with collision avoidance (CA) in the form of CTS and RTS handshaking packets. The RTS and CTS packets warn nodes within range of the source and destination to delay future transmissions until the current transaction finishes. Since I-UWB requires a relatively long acquisition time, the RTS and CTS packets can create significant overhead [13]. Amortizing the cost of the RTS/CTS preambles over longer data packets may not resolve this problem, since larger data packets incur more bit errors.

III. PROPOSED RADIO AND MAC

To manage collisions, a random access protocol time-multiplexes handshaking packets with data packets. A more efficient approach in terms of channel utilization is to provide

feedback *during* data transmission. Busy signal MAC protocols use this feature to reduce overhead, to increase throughput, and to efficiently manage collisions. Since a transmitter immediately knows of a collision, it wastes less energy transmitting corrupted packets. This section describes our *single* I-UWB transceiver architecture that enables a busy signal protocol. It also reviews applicable busy tone protocols and develops criteria for system design.

A. System Architecture

To implement a busy signal, a transceiver must be capable of full duplex operation [18]. Narrowband radios implement full duplex operation with two transceivers in different frequency bands. The proposed I-UWB system requires only a single transceiver, but achieves nearly full duplex through a fine-grained half duplex. This is possible because an I-UWB signal is not continuously transmitted like a narrowband signal. The proposed I-UWB radio exploits the idle time between pulses to assess the state of its transmission. Note that both the data signal and the busy signal are in the same band and share the same RF circuitry.

Fig. 3 compares time division duplex (TDD), frequency division duplex (FDD), and fine-grained half duplex with I-UWB. The TDD system in Fig. 3 (a) cannot simultaneously transmit and receive, so it incurs penalties in latency and data rate. The TDD system also adds delay from the propagation time and from the turnaround time, or the time to switch from transmit mode to receive mode. The FDD system in Fig. 3 (b) can transmit and receive simultaneously, but it requires an additional frequency band for the feedback channel. The I-UWB system in Fig. 3 (c) achieves full duplex without the latency or speed penalty of the TDD system and without the additional frequency band of the FDD system. An I-UWB system performs the following operations for the fine-grained half duplex. Starting in the receive mode, it receives a pulse. Then it switches from receive mode to transmit mode and transmits a pulse. After transmitting, it switches back to receive mode, and it is ready to receive the next pulse.

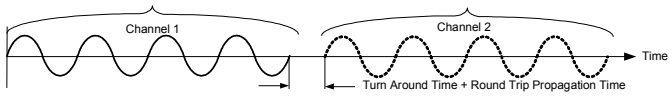

(a) Time Division Duplex

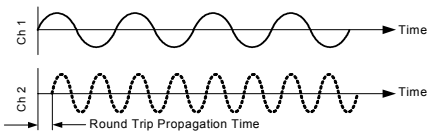

(b) Frequency Division Duplex

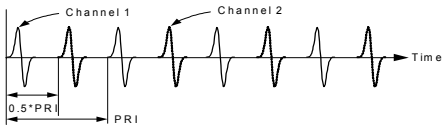

(c) Fine-Grained Time Division Half Duplex with I-UWB

Fig. 3. Types of Duplexing

Fig. 4 compares an FDD architecture to the proposed fine-grained half duplex I-UWB architecture. Fig. 4 (a) shows an architecture for narrowband FDD full duplex in ad hoc networks. It requires two transceivers and circulators for the two different frequency bands. An ad hoc network has no base station to translate between frequency bands for inter-node communication. Therefore, each node must be able to receive and transmit in either band, depending if it is a source node or a destination node. In addition, the feedback channel requires an additional frequency band to degrade spectral efficiency.

Fig. 4 (b) shows the proposed architecture for I-UWB with fine-grained half duplex. A low duty allows a single transceiver to access a feedback channel in the same frequency band as the transmitted data. The switching time between transmit and receive modes determines the minimum pulse repetition interval. Instead of using a typical T/R switch, we switch the disable inputs to the PA and the LNA. This scheme improves the switching time to 250 ps and results in no additional noise figure like a T/R switch. It also provides the necessary isolation, since there is very little leakage into the PA and LNA when they are disabled. The fine-grained half duplex I-UWB transceiver significantly reduces circuit cost and increases spectral efficiency as compared to a narrowband FDD transceiver.

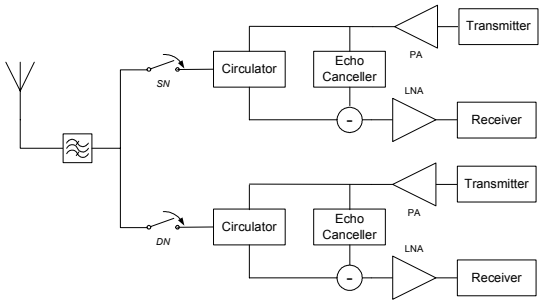

(a) System Architecture for Frequency Domain Division Full Duplex

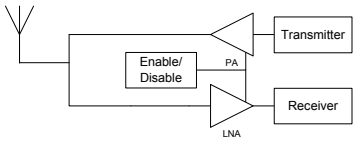

(b) Fine-Grained Time Domain Half Duplex with I-UWB

Fig. 4. Full Duplex System Architectures for Ad Hoc Radios

B. Busy Signal Protocol

A busy signal provides two services: (i) to inform the source node of a successful (or unsuccessful) transmission and (ii) to prevent nodes within radio range of the destination node from initiating a transmission. The busy signal eliminates control packets such as RTS, CTS, and ACK, so they do not incur synchronization overhead or require fast turnaround time between transmit and receive mode [14]. This efficiently manages collisions and increases throughput as compared to a handshaking protocol. Further, the busy signal immediately alerts the source node to a dropped packet or a collision, thus resulting in few wasted transmissions. Finally, a busy signal

prevents hidden terminals and can also prevent exposed terminals [14]. We briefly review some varieties of busy-tone multiple access (BTMA) that our I-UWB radios can support.

In basic BTMA, any node that detects a transmission emits a busy signal to prevent nodes within 2*R* range (where *R* is the transmit range of a node) of the source node from transmitting [19]. This eliminates hidden nodes but increases the number of exposed nodes.

Receiver initiated BTMA (RI-BTMA) requires the destination node to emit a busy signal after it decodes its address [20]. Therefore, nodes within radius *R* of the destination are prevented from transmitting, resulting in fewer exposed nodes. However, this results in a long vulnerable period before the address is decoded.

Finally, wireless collision detect (WCD) combines RI-BTMA and BTMA [14]. During the preamble, all nodes within radius 2*R* of the source node emit a busy signal. After the destination node decodes its address, the other nodes terminate their busy signals, and only the destination node emits a busy signal. WCD allows exposed nodes to transmit after the preamble as in RI-BTMA, but without the long vulnerable period.

The above BTMA protocols can leverage the low transmit power of I-UWB by transmitting the busy signal for the duration of the transaction, while the source node only periodically checks for a busy signal.

C. Design Goals

This section develops two important design goals to support a busy signal. The system should: (i) not degrade data reception at the destination node and (ii) be easily detectable [14].

Self-interference complicates the above design goals. After transmitting a busy signal, the multipath channel causes a long ring down time, and some of the busy signal multipaths could interfere with data reception. Further, when multiple receivers emit a busy signal, they may interfere with data reception at the destination and busy signal detection at the source.

The phenomenon of *overlap* may also degrade performance [18]. Depending on the flight time, a busy signal pulse may overlap a data pulse at either the source or the destination. For clarity, we assume the overlap occurs at the source node, and the destination node is free to transmit the busy signal so as to avoid overlap. Thus, depending on the link distance, a portion of the busy signal (including multipaths) may arrive while the source node transmits a data pulse.

Fig. 5 illustrates the occurrence of overlap as link distance changes. At Time 1, the source node transmits a pulse, which arrives one propagation time, T_{prop}, later at the destination node at Time 2. At Time 3, the destination node sends a busy signal pulse exactly $0.5 \cdot PRI$ after the arrival of the first data pulse. Finally, at Time 4, the source node receives the busy signal pulse from the destination node.

In Fig. 5 (a), the destination node is distance $d = c \cdot PRI$ meters (e.g., for a PRI of 100 ns, this distance is 30 meters) from the source node, so the round trip propagation time is $2 \cdot PRI$. Therefore, a busy signal pulse arrives exactly $2.5 \cdot PRI$ after the corresponding data pulse. In Fig. 5 (b), the busy signal pulse overlaps the data transmission. The destination node is distance $d = 0.75 \cdot c \cdot PRI$ meters from the source node; the round trip propagation time is $1.5 \cdot PRI$; and the busy signal pulse arrives exactly $2 \cdot PRI$ after the corresponding data pulse. Since the source node is transmitting at the time, it loses some energy from the busy signal. Note that Fig. 5 shows only the first multipath of a received pulse. In real-world situations, a receiver could detect a significant portion of the multipath energy.

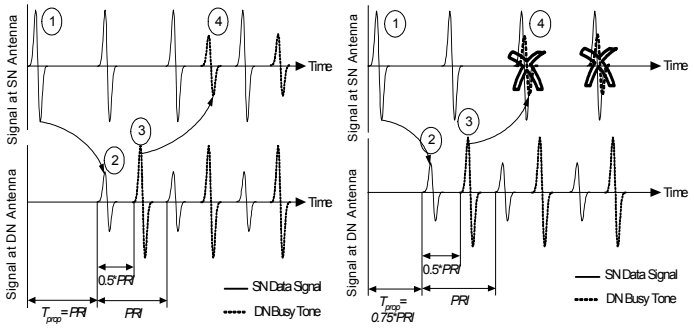

(a) Distance = $c*PRI$ (b) Distance = $0.75*c*PRI$

Fig. 5. Overlap Effect

1) Source Node: The goal of transceiver design from the source node perspective is to detect a busy signal while rejecting noise, other data transmissions, and its own self-interference from the received signal R_{SN}.

$$R_{SN}(t) = x_i(t) * \left[\sum_j b_j(t - t_{j,SN}) * h_{j,SN}(t) + \sum_k s_k(t - t_{k,SN}) * h_{k,SN}(t) + n(t) \right] + x_i(t) * s_{SN}(t - t_d) \quad (1)$$

where

$b_j(t)$	busy signal from node j, including destination node, $j \neq$ source node, $j \neq k$
$h_{j,SN}(t)$	channel response node j to the source node
$x_i(t)$	impulse response of the switch in state $i \in$ (Rx, Tx) including ringing
$s_{SN}(t)$	data signal from the source node
t_d	delay to the switch
$t_{j,SN}$	propagation delay from node j to the source node
$t_{k,SN}$	propagation delay from node k to the source node
$s_k(t)$	data transmission from node k, including source node, $k \neq$ destination node, $k \neq j$
$h_{k,SN}(t)$	channel response from node k to the source node
$n(t)$	the noise at the destination node receiver

The source performs a sliding correlation with result

$$C_m = \int R_{SN}(t) \cdot b(t - t_m)\, dt \quad (2)$$

where $t_m \in [0, PRI + T_p]$ and is changing uniformly each PRI by $(PRI + T_p) / k$, with k the number of sliding correlations. To optimally detect a busy signal in noise, conditions (3), (4), and (5) should be true.

$$\int x_i(t) * s_{SN}(t - t_d) \cdot b(t - t_m)\, dt = 0 \quad (3)$$

$$\int \left[x_i(t) * \sum_k s_k(t) * h_{k,SN}(t) \right] \cdot b(t - t_m)\, dt = 0 \quad (4)$$

$$\int x_i(t) * \sum_j b_j(t) * h_{j,SN}(t) \cdot b(t - t_m)\, dt = C_{\max} \quad (5)$$

Condition (3) is satisfied if either: (i) the data transmission does not overlap in time with the receiver operation or (ii) the switch can perfectly separate the transmitted pulse from the receiver chain. Since I-UWB signals are not continuous, they can satisfy condition (3) with one transceiver. Condition (4) requires data from other transmitters and multipaths from the source node to arrive at a different time than the busy signal at the source node. Since this is difficult to control, the busy signal should be separated from the data signal. This can be achieved with an orthogonal pulse shape or through spreading techniques such as direct sequence UWB (DS-UWB). Condition (5) means that the transceiver should capture as much busy signal energy as possible. Further, a busy signal should not combine destructively with other busy signals.

2) Destination Node: The goal of transceiver design from the destination node perspective is to demodulate the data signal, while rejecting noise, other busy signal transmissions, and self-interference from the received signal R_{DN}.

$$R_{DN}(t) = x_i(t) * \left[s_{SN}(t - t_{SN,DN}) * h_{SN,DN}(t) + \sum_j b_j(t - t_{j,DN}) * h_{j,DN}(t) + n(t) \right] + x_i(t) * b_{DN}(t - t_d) \quad (6)$$

where

$b_j(t)$	busy signal from node *j,* including destination node, $j \neq$ source node, within range of destination node
$b_{DN}(t)$	busy signal from the destination node
$h_{j,DN}(t)$	channel response from node *j* to the destination node
$x_i(t)$	impulse response of the switch in state $i \in$ (Rx, Tx) including ringing
$s_{SN}(t)$	data signal from the source node
t_d	delay to the switch
$t_{SN,DN}$	propagation delay from the source node to the destination node
$t_{j,DN}$	propagation delay from node *j* to the destination node
$h_{SN,DN}(t)$	channel response from the source node to the destination node
$n(t)$	the noise at the destination node receiver

Assuming coherent detection, the destination node performs the following correlation on the received signal, where s_n is the n^{th} basis function of the signal set.

$$C_n = \int R_{DN}(t) \cdot s_n(t)\, dt \quad (7)$$

To optimally detect the data in noise, conditions (8), (9), and (10) should be true.

$$\int x_i(t) * b_{DN}(t - t_d) \cdot s_n(t)\, dt = 0 \quad (8)$$

$$\int \left[x_i(t) * \sum_j b_j(t) * h_{j,DN}(t) \right] \cdot s_n(t)\, dt = 0 \quad (9)$$

$$\int x_i(t) * s_{SN}(t) * h_{SN,DN}(t) \cdot s_n(t)\, dt = C_{\max} \quad (10)$$

To satisfy condition (8), the destination node's busy signal should not interfere with reception. Condition (9) requires the busy signal pulses from other nodes to not interfere with reception, so busy signal pulses should be separated from data pulses as for the source node. Condition (10) means that the transceiver should capture as much of the received data signal energy as possible.

Finally, a node that is neither the source nor the destination must accurately detect a busy signal. This situation is similar to that of a source node detecting a busy signal without overlap.

IV. Simulation Results

We compare the performance of the following methods to meet the criteria in Section III.

1) Use different PRIs for the data signal and the busy signal. If $PRI_{data\ signal}$ is $n*PRI_{busy\ signal}$, for an integer n, then the source node can detect either n or n-1 busy signal pulses, each having a power of $1/n$ of the data signal. Alternately, if $PRI_{busy\ signal}$ is slightly less than the $PRI_{data\ signal}$, then the pulses will only overlap at some small beat frequency [18].
2) Use different waveforms for the data signal and the busy signal, e.g. DS-UWB and I-UWB. Also, orthogonal pulse shapes can differentiate the busy signal from the data, e.g. a Gaussian monopulse and the first derivative of a Gaussian monopulse are orthogonal.
3) Rely on multipath effects to detect the busy signal. The multipath spread of an I-UWB signal can be quite significant compared to the pulse length. The source receiver is disabled during transmission, but energy from busy signal multipaths arrives for a period much longer than the data pulse width.
4) Estimate and equalize the channel. A destination node can estimate and subtract its own busy signal reflections and the busy signal of other nodes from the received data. A source node can also estimate the reflections from its own data, but this is more complicated in hardware due to the modulation.
5) Use a PRI at least twice the maximum propagation time plus twice the multipath delay spread. After receiving a data pulse, the destination node waits for a period of time equal to the multipath delay spread before transmitting a busy signal pulse. Likewise, after detecting a busy signal pulse, the source node waits for a multipath delay spread before transmitting data. If the PRI is such that $PRI \geq 2 \cdot (R_{max}/c + D_{multipath})$, then the system avoids interference. For a range R_{max} of 30 m and multipath delay spread $D_{multipath}$ of 200 ns, the minimum PRI is 600 ns. The maximum pulse rate becomes 1.67 Mpps, which is sufficient for most low data rate networks.

To show the feasibility of the proposed I-UWB transceiver for a busy signal protocol, we compare the above methods from the perspective of a source node and a destination node. For

simulation, the network topology is random with multihop connections. Each node has an average of about 6 neighbors with a maximum link distance of 10 m. The channel model is based on the Cassioli channel model for indoor UWB propagation [21], and it considers statistical variations in small scale and large scale fading and shadowing. Fig. 6 displays the average power delay profile. Time is relative to the first arriving multipath, and the amplitude of each vertical line represents the energy gain during a 2 ns delay bin. A multipath "dies out" if its power is less than 6 dB above the noise floor. On average, 11% of total energy arrives in the first multipath, 57% arrives after 30 ns, and 92% arrives within 100 ns. Each transaction results in a different, random instance of the channel model and the topology. The average of 100 simulations results in each data point.

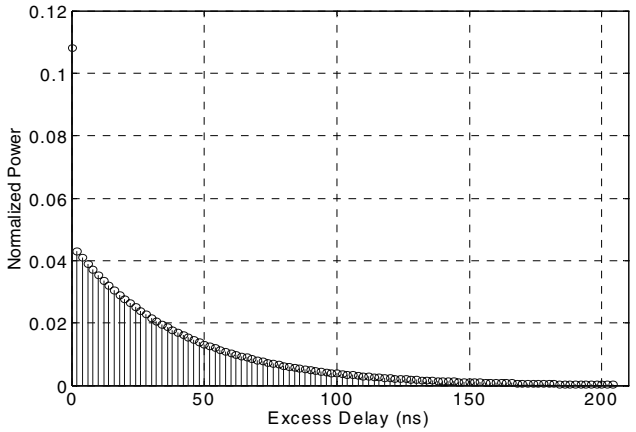

Fig. 6. Average Power Delay Profile of the Channel

TABLE I. SIGNALS USED IN THE SIMULATIONS

Name	Description
Data	The data signal. BPSK modulation. Uncoded.
1 Pulse	Busy Signal with the same PRI and energy as the data signal.
Divided PRI	Busy signal. Each pulse has $1/n^{th}$ the energy and $1/n^{th}$ PRI of a data pulse.
2 Pulses	*Divided PRI* busy signal with n=2.
4 Pulses	*Divided PRI* busy signal with n=4.
Different PRI	Busy Signal. Each pulse has the same energy as a data pulse, but the PRI is 99.5% of the data signal PRI to result in a beat frequency of 200/PRI.
DS-UWB	Busy signal with spreading factor = *SF*. Each pulse has 1/*SF* the energy of a data pulse. The chips are transmitted back to back and each bit is separated by the PRI of the data signal.
8 DS-UWB	*DS-UWB* with *SF*=8.
16 DS-UWB	*DS-UWB* with *SF*=16.
32 DS-UWB	*DS-UWB* with *SF*=32.

The source node performance is measured by the probability of false alarm (P_{FA}) vs. the probability of detecting the busy signal (P_D). The destination node performance is measured by the noise that the busy signal adds to the received data signal. Table 1 describes the signals used in simulation.

A. Source Node Results

To show the accuracy of the proposed system in detecting a busy signal without constraining the PRI (as in Method 5), we plot the probability of detection vs. the probability of false alarm for a data rate of 100 Mbps under various conditions of interference. Assuming an 11 dB noise figure at the receiver, we adjust the busy signal power such that the strongest received multipath has a maximum SNR of 4 dB, which just meets the FCC limits at a 10 m link distance. Better performance may be achieved with multiple "looks," lower data rates, and shorter distances. The figures compare the relative performance of the different methods.

For the ideal case of Method 5, the top graph of Fig. 7 (a) shows the performance of the busy signal detection with the line labeled *Clear Channel*, which serves as a reference line in the remaining graphs. The other lines show the performance for a busy signal that arrives with 3 dB less power than the data signal reflections. Additionally, there is no overlap in Fig. 7. This situation also corresponds to that of an idle node.

Fig. 7 (a) does not include the *Different PRI* busy signal, since it is guaranteed to overlap the transmission periodically. The best performing busy signal is the *4 Pulse*, since it spreads four pulses evenly over the PRI. In the worst case, only one pulse out of four experiences severe interference. The *2 Pulse* busy signal performs next best, as it also spreads its pulses over the PRI; but now half the pulses may experience severe interference. Next, the *DS-UWB* signals (all spreading factors performed similarly) perform almost as well as the *2 Pulse* and *4 Pulse* signals, since the spreading code combats interference. However, since the chips are sent consecutively, the data signal interferes with all the chips, and hence performance is not as good a *2 Pulse* or *4 Pulse*. Finally, the *1 Pulse* busy signal performs the worst, since it has no method to combat interference. All busy signals result in little performance degradation as compared to the ideal case, since the receiver only needs to detect the presence of a busy signal.

Nonlinear effects from the antenna, channel, and RF circuitry may cause the busy signal and the data signal to lose orthogonality. Fig. 7 (b) shows that performance degradation is still mild even when the data signal and the busy signal have identical pulse shapes.

Finally, we simulated the performance of each busy signal when the receiver estimates its self-interference from the data signal and equalizes it. The hardware complexity increases but the performance is indistinguishable from the ideal *Clear Channel* case as shown in Fig. 7 (c).

Fig. 8 shows the performance of each busy signal when the strongest multipaths overlap the data signal transmission. The overlap consists of a 1 ns transmission, two 0.25 ns T/R switches, and an additional 0.5 ns of settling time for a total of 2 ns. The busy signal arrives with 3 dB less power than the data signal reflections, and the overlap causes an average loss of about 10% of the total busy signal energy.

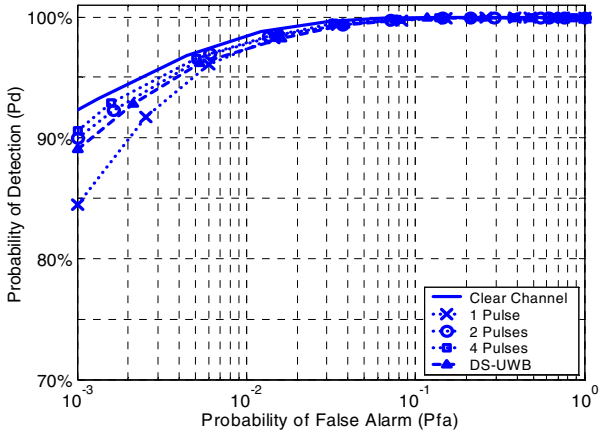

(a) Data Signal Orthogonal to Busy Signal, No Equalization

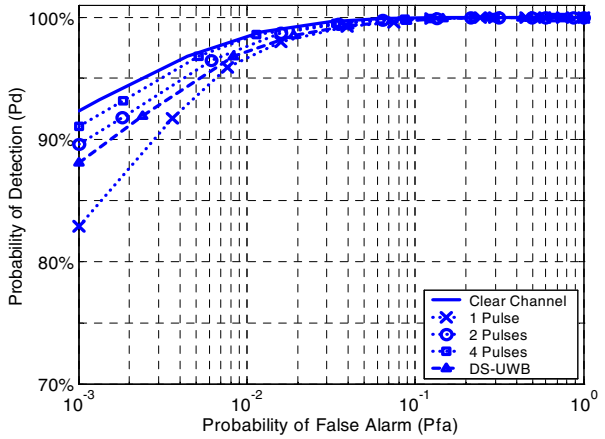

(b) Data Signal Non-Orthogonal to Busy Signal, No Equalization

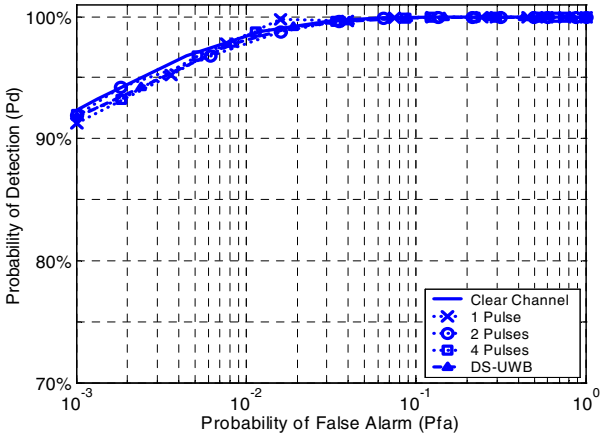

(c) Data Signal Orthogonal to Busy Signal, Equalization

Fig. 7. P_D vs. P_{FA} for Busy Signals with Interference

Fig. 8 (a) shows the performance without channel estimation and equalization. The *Different PRI* busy signal performs best in these conditions, since it overlaps the data signal transmission only periodically. The next best signal is the *32 DS-UWB*, since the spreading code is long, and the source node

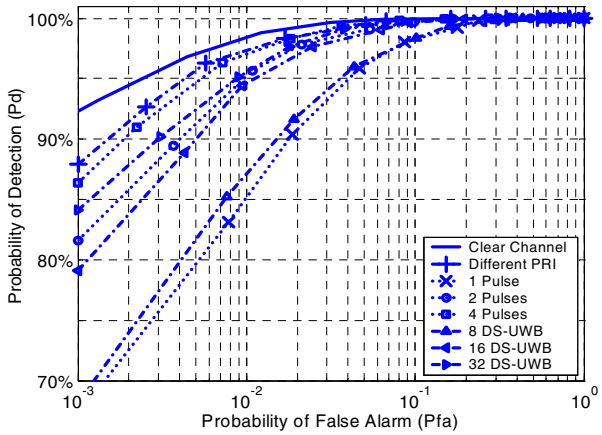

(a) No Equalization

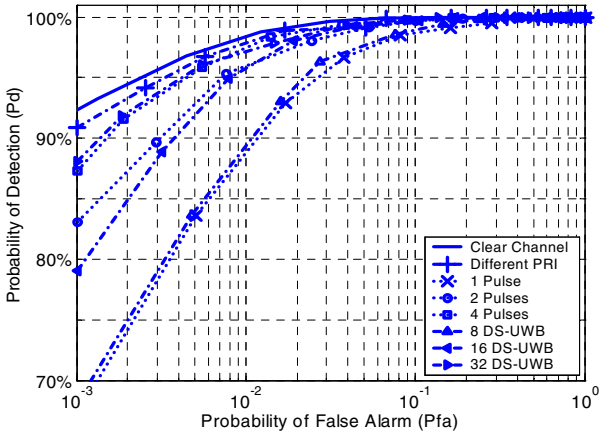

(b) Equalization

Fig. 8. P_D vs. P_{FA} for Orthogonal Busy Signals with Interference and Overlap

receiver loses a smaller portion of energy due to overlap. The *16 DS-UWB* signal loses twice as much energy as compared to the *32 DS-UWB* signal, and the *8 DS-UWB* signal loses four times as much energy. Hence, higher spreading gain improves performance under the conditions of overlap. The *4 Pulse* busy signal performs similarly to *32 DS-UWB* since it spreads four pulses evenly over the data PRI. The receiver loses energy from only one the pulses due to overlap. The *2 Pulse* busy signal suffers more degradation than the *4 Pulse* case, since the overlapped pulse loses twice as much energy. Finally, the *1 Pulse* busy signal performs the worst, since it has no method to offset the effects of overlap. The *Different PRI*, *Divided PRI* with larger *n*, and the *DS-UWB* with larger *SF* result in mild degradation of the performance as compared to the ideal case. They all combat the effects of overlap.

Fig. 8 (b) displays the performance of each busy signal when the receiver estimates its self-reflected channel and equalizes the interference. As compared to Fig. 8 (a), the performance improves slightly at the cost of increased hardware complexity and power. The performance gain is limited, since the busy signal that overlaps with data transmission is unrecoverable.

Fig. 9 shows the performance when multiple nodes emit busy signals. Six neighbors emit a busy signal, and they are

uniformly distributed around the source node. The busy signals interfere with each other and may combine destructively. The received busy signal also overlaps the data transmission and is corrupted by the data signal multipaths. The total interference results in a busy signal to interference ratio of –7 dB, and the overlap loss averages about 10% of busy signal energy.

The performance of the *Different PRI* busy signal is worse than the single busy signal case, since all the busy signals experience overlap and interference periodically. The *4 Pulse* and *2 Pulse* busy signals improve performance as compared to the single busy signal. Additional energy from one of the other busy tones may experience more favorable channel conditions. The *1 Pulse* busy signal improves performance the most. The pulses appear in a narrower time window and are less likely to combine destructively. The best performing signal is the *32 DS-UWB* busy signal, since the spreading code is long, and it combats both overlap and destructive combination. The *Different PRI*, *Divided PRI* with larger *n*, and the *DS-UWB* with larger *SF* all combat the interference from multiple busy signals.

For DS-UWB, the spreading code should be chosen to minimize autocorrelation, since the busy signals may overlap and combine destructively. Fig. 9 shows simulation results in which an *m*-sequence code is used. Fig. 9 also shows the performance degradation for *32 DS-UWB* with a random, rather than an *m*-sequence code. Degradation increases for longer codes, as busy tones are more likely to overlap.

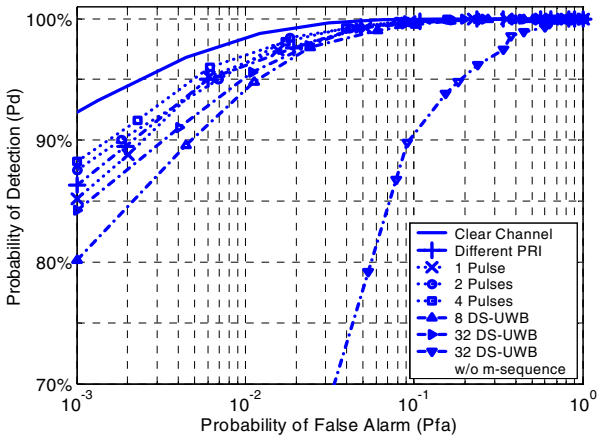

Fig. 9. P_D vs. P_{FA} for Multiple Busy Signals

B. Destination Node Results

We simulate the busy signals in Table I to determine their impact on data reception as the PRI decreases. For each busy signal, we simulate with three representative topologies that result in SINRs of 3 dB, 0 dB, and -3 dB as the link distance changes. We present the results in terms of noise figures, and the effect on BER will depend on various factors including link distance, receiver type, and coding. For reference, in the worst simulation case, 1 dB of noise increases the BER from 2×10^{-4} to 8×10^{-4}, and 0.5 dB of noise increases the BER to 3×10^{-4}.

Fig. 10 shows the noise that each busy signal adds to the data signal for the three topologies. The *Different PRI* busy signal performs worst, since its pulses are guaranteed to periodically occur close in time to the beginning of a receive cycle. The *1 Pulse* busy signal results in the least additional noise since it transmits all busy signal energy immediately after a receive cycle, thus allowing the most ring down time before the next receive cycle. The *2 Pulse* busy signal performs slightly worse than the *1 Pulse* case for short PRI, since the reduced power of the second pulse does not offset the fact that it appears closer to the beginning of the next receive cycle. Finally *8 DS-UWB* performs similarly to *1 Pulse*, since it is also transmitted immediately following a receive cycle. All busy signals add noise to the received signal at short PRIs, so a designer may adjust the PRI to meet link budget constraints.

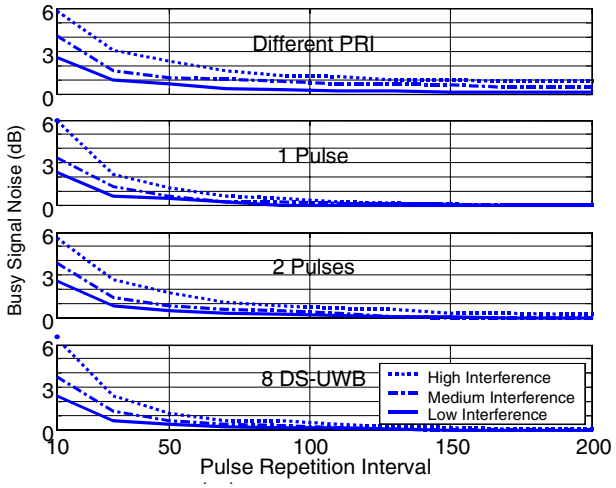

Fig. 10. Busy Signal Noise for Different Levels of Interference

Fig. 11 shows the effect of increasing the spreading factor for both *Divided PRI* and *DS-UWB*. The *Divided PRI* signal adds noise as the number of pulses *n* increases. Although the signal power decreases with *n*, more busy signal energy occurs near the beginning of the next receive cycle. The *DS-UWB* signal does not incur any penalty as compared to the *1 Pulse* case for any spreading factor. This is because the destination node transmits the *DS-UWB* busy signal immediately after the receive cycle, so it contributes less interference to the next receive cycle.

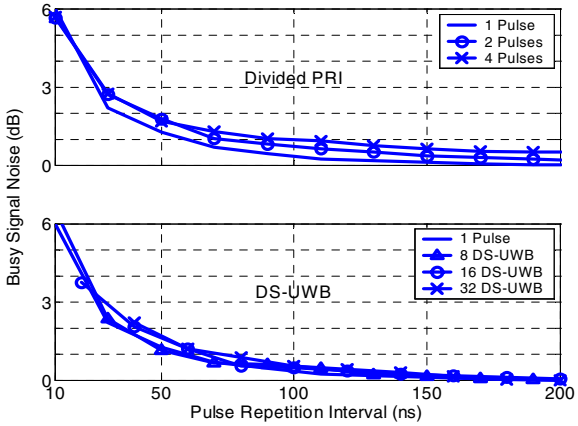

Fig. 11. Busy Signal Noise for Different Spreading Factors

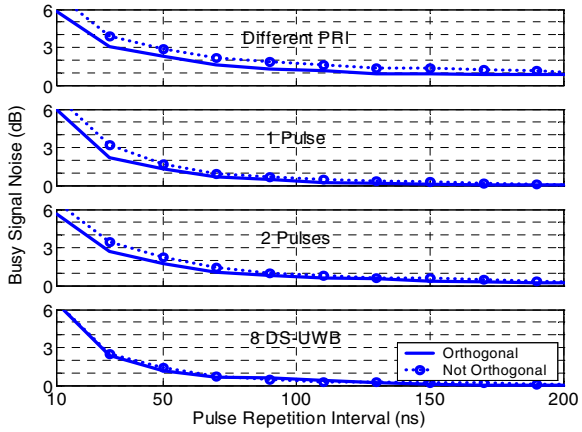

Fig. 12. Busy Signal Noise for Different Pulse Shapes

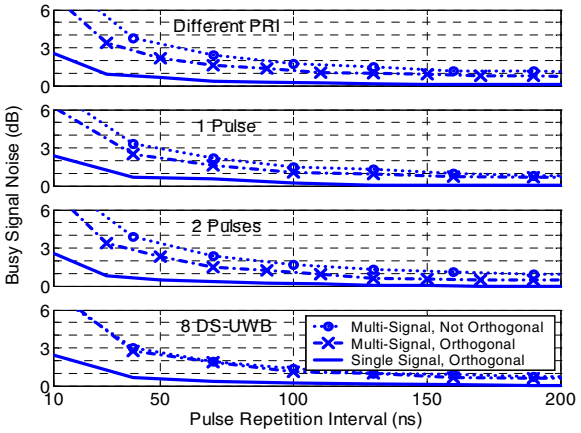

Fig. 13. Busy Signal Noise for Different Busy Signal Protocols

Since the antenna, channel, and receiver front-end may introduce non-linear effects into the received signal, the busy signal and data signal pulses may lose orthogonality. Fig. 12 shows the simulation results for a busy signal pulse shape that is identical to the data pulse shape under the highest level of self-interference. The *Different PRI* busy signal adds from 0.5 dB to 1 dB of noise. The *1 Pulse* busy signal adds noise at shorter PRIs, since longer PRIs allow the multipath reflections to ring down. The *2 Pulses* busy signal adds slightly more noise than the *1 Pulse* busy signal due to the closer proximity of the second busy signal pulse to the beginning of the next receive cycle. Finally, the *8 DS-UWB* signal incurs negligible additional interference due to the spreading gain. In all cases, the effects of non-orthogonal signals are moderate, and the total energy in the channel has a greater impact on performance.

Fig. 13 shows the effects of multiple nodes emitting a busy signal. Six neighbors with a uniform, random distribution of distances emit a busy signal. Each graph compares a single busy signal with low self-interference to multiple busy signals with low self-interference. For all cases, the multiple busy signals add significantly more noise than a single busy signal. This is because the source node cannot control the time at which it receives the busy signals from other nodes. For the three cases of *Different PRI*, *1 Pulse*, and *2 Pulses*, the loss of orthoganality is more significant than the case with just one node. However, the *DS-UWB* busy signal still performs as well as the orthogonal case.

Finally, we simulate the effects of channel estimation and equalization on data reception. The estimation and equalization process is relatively simple, since the busy signal is known and it never changes. The simulation uses 8-bit quantization of seven frequency domain samples. Equalization dramatically reduces noise at shorter PRIs but adds small quantization noise at longer PRIs. Fig. 14 shows that the quantization noise averages about 0.2 dB for both single and multiple busy tones. The channel estimation scheme improves performance at the expense of additional hardware and power.

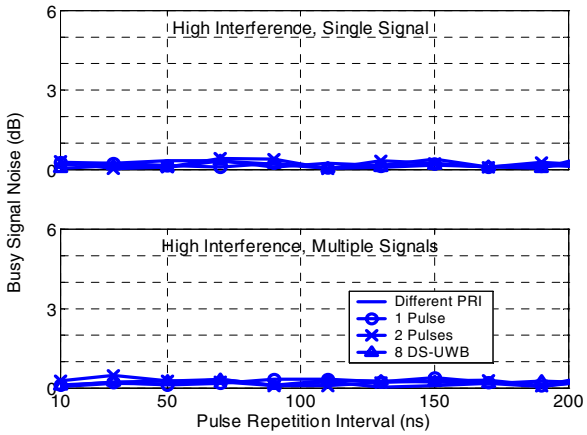

Fig. 14. Busy Signal Noise with Equalization Scheme

V. Conclusion

For ad hoc and sensor networks, low node cost and low power dissipation are essential design considerations. The MAC protocol and the radio play a crucial role in determining both the node cost and the amount of energy spent on a successful transmission.

I-UWB is a particularly attractive radio for ad hoc and sensor networks due to its resilience to multipath interference, simple transceiver circuitry, accurate ranging ability, and low transmission power. Further I-UWB enables a single transceiver architecture for a MAC based on busy signals. Such a MAC provides performance similar to CSMA/CD, which is more efficient than CSMA/CA in throughput, delay, and energy per successful transmission [14]. It also permits random, distributed medium access with no central point of failure, so it is appropriate for any large ad hoc or sensor network.

The single transceiver leverages the inherently low duty cycle of an I-UWB pulse train to detect collisions and corrupted packets through a busy signal. The busy signal avoids the overhead of time-duplexed control packets. The

system finely multiplexes the busy signal channel with the data channel to re-use the same frequency band and radio front end. Further, I-UWB systems dissipate far less power transmitting than receiving, so the busy signal does not significantly increase power.

At the cost of lower data rate, the simplest and most effective method of implementing the busy signal is to set the PRI long enough to avoid any interference. At shorter PRIs, the simulations find that channel estimation at both the source node and the destination node provides comparable performance at the cost of additional hardware. To implement the busy signal without increased hardware complexity, an orthogonal *DS-UWB* signal with a high spreading gain incurs only a slight degradation of BER at the destination node, and it is easily detected at the source node.

REFERENCES

[1] A. Woo and D. E. Culler, "A transmission control scheme for media access in sensor networks," Proceedings of the 7th annual international conference on Mobile computing and networking, pp.221-235, July 2001, Rome, Italy.

[2] J.-P. Hubaux, J.-Y. Le Boudec, S. Giordano, M. Hamdi, L. Blazevic, L. Buttyan, M. Vojnovic, "Towards mobile ad-hoc WANs: terminodes," Proceedings Wireless Communications and Networking Conference, 2000," vol. 3, pp. 1052 – 1059, Sep. 2000.

[3] The Institute of Electrical and Electronics Engineers, Inc., IEEE Std 802.11 - Wireless LAN Medium Access Control (MAC) and Physical Layer (PHY) Specifications, 1999 edition.

[4] M. Leopold, M.B. Dydensborg, and Philippe Bonnet, "Bluetooth and Sensor Networks: A Reality Check," Proceedings of the first ACM International Conference on Embedded Networked Sensor Systems (SenSys), pp. 103-113, November 2003.

[5] O. Kasten and M. Lamgheinreich, "First Experiences with Bluetooth in the Smart-ITS distributed Sensor Network," In Workshop on Ubiquitous Computing and Communications, PACT, 2001.

[6] Macro Motes of Smart Dust Project available at http://www-bsac.eecs.berkeley.edu/archive/users/hollar-seth/macro_motes/macromotes.html.

[7] Y. Wei, J. Heidemann, and D. Estrin, "An energy-efficient MAC protocol for wireless sensor networks," Proceedings of INFOCOM 2002. Twenty-First Annual Joint Conference of the IEEE Computer and Communications Societies. pp. 1567-1576, vol. 3, June 2002.

[8] I.F. Akyildiz et al., "A Survey on Sensor Networks," IEEE Communications Magazine, pp.102-114, August 2002.

[9] F. Legrand, "Motivation in 15.4a," IEEE802.15.4a Task Group presentation, ftp://ieee:wireless@ftp.802wirelessworld.com/15/04/15-04-0119-00-004a-thales-coms-motivation-in-ieee-802-15-4a.ppt, March 2004.

[10] H.-J. Lee, D.S. Ha, and H.-S. Lee, "A Frequency-Domain Approach for All-Digital CMOS Ultra Wideband Receivers," IEEE Conference on Ultra Wideband Systems and Technologies, pp. 86-90, November 2003.

[11] K. Marsden, H.-J. Lee, D.S. Ha, and H.-S. Lee, "Low Power CMOS Re-programmable Pulse Generator for UWB Systems," IEEE Conference on Ultra Wideband Systems and Technologies, pp. 443-337, November 2003.

[12] W. C. Chung and D. S. Ha, "An accurate ultra wideband (UWB) ranging for precision asset location," 2003 IEEE Conference on Ultra Wideband Systems and Technologies Conference Proceedings, pp. 389-393, Nov. 2003.

[13] J. Ding, L. Zhao, S. Medidi, and K. Sivalingam, "MAC Protocols for Ultra-Wide-Band (UWB) Wireless Networks: Impact and Channel Acquisition Time," Proc. SPIE ITCOM02, July 2002.

[14] A.C.V. Gummalla and J.O. Limb, "Design of an access mechanism for a high speed distributed wireless LAN," IEEE Journal on Selected Areas in Communications, vol. 18, no. 9, pp. 1740-1750, Sep. 2000.

[15] N.J August, H.J. Lee, and D.S. Ha, "Pulse Sense: A method to detect a busy medium in ultra wideband (UWB) networks," Digest of Papers. 2004 Joint IEEE Conference on Ultra Wideband Systems and Technologies and International Workshop on UWB Systems, pp. 314-318, May 2004.

[16] R. Scholtz, "Multiple access with time hopping impulse modulation," Conference Record of the IEEE Military Communications Conference, vol. 2 pp. 447-450, Oct 1993.

[17] The Institute of Electrical and Electronics Engineers, Inc., 802.15.3 Draft Standard for Telecommunications and Information Exchange Between Systems - LAN/MAN Specific Requirements - Part 15: Wireless Medium Access Control (MAC) and Physical Layer (PHY) Specifications for High Rate Wireless Personal Area Networks, Draft P802.15.3/D17, Feb. 2003.

[18] L.W. Fullerton, "Full duplex ultrawide-band communication system and method," U.S. Patent 5 687 169, Nov. 11, 1997.

[19] F. Tobagi and L. Kleinrock, "Packet switching in radio channels: part II--the hidden terminal problem in carrier sense multiple-access and the busy-tone solution," IEEE Transactions on Communications, vol. 23, no. 12, pp. 1417-1433, Dec 1975.

[20] C. Wu and V. Li, "Receiver-initiated busy-tone multiple access in packet radio networks," Proceedings of the ACM Workshop on Frontiers in Computer Communications Technology, p.336-342, August 11-13, 1987, Stowe, Vermont, United States.

[21] D.Cassioli, M.Z. Win, and A.F. Molisch, "The ultra-wide bandwidth indoor channel: from statistical model to simulations," IEEE Journal on Selected Areas in Communications, Vol. 20, No. 6, pp. 1247-1257, Aug. 2002.